Clean Energy, 2024, Vol. 8, No. 5, 157–166
https://doi.org/10.1093/ce/zkae060
Advance access publication 27 August 2024
Research Article

Hybrid firefly algorithm–neural network for battery remaining useful life estimation

Zuriani Mustaffa[1,*] and Mohd Herwan Sulaiman[2]

[1]Faculty of Computing, Universiti Malaysia Pahang Al-Sultan Abdullah (UMPSA), 26600 Pekan Pahang, Malaysia
[2]Faculty of Electrical & Electronics Engineering Technology, Universiti Malaysia Pahang Al-Sultan Abdullah (UMPSA), 26600 Pekan Pahang, Malaysia
*Corresponding author. E-mail: zuriani@umpsa.edu.my

Abstract

Accurately estimating the remaining useful life (RUL) of batteries is crucial for optimizing maintenance, preventing failures, and enhancing reliability, thereby saving costs and resources. This study introduces a hybrid approach for estimating the RUL of a battery based on the firefly algorithm–neural network (FA–NN) model, in which the FA is employed as an optimizer to fine-tune the network weights and hidden layer biases in the NN. The performance of the FA–NN is comprehensively compared against two hybrid models, namely the harmony search algorithm (HSA)–NN and cultural algorithm (CA)–NN, as well as a single model, namely the autoregressive integrated moving average (ARIMA). The comparative analysis is based mean absolute error (MAE) and root mean squared error (RMSE). Findings reveal that the FA–NN outperforms the HSA–NN, CA–NN, and ARIMA in both employed metrics, demonstrating superior predictive capabilities for estimating the RUL of a battery. Specifically, the FA–NN achieved a MAE of 2.5371 and a RMSE of 2.9488 compared with the HSA–NN with a MAE of 22.0583 and RMSE of 34.5154, the CA–NN with a MAE of 9.1189 and RMSE of 22.4646, and the ARIMA with a MAE of 494.6275 and RMSE of 584.3098. Additionally, the FA–NN exhibits significantly smaller maximum errors at 34.3737 compared with the HSA–NN at 490.3125, the CA–NN at 827.0163, and the ARIMA at 1.16e + 03, further emphasizing its robust performance in minimizing prediction inaccuracies. This study offers important insights into battery health management, showing that the proposed method is a promising solution for precise RUL predictions.

Graphical Abstract

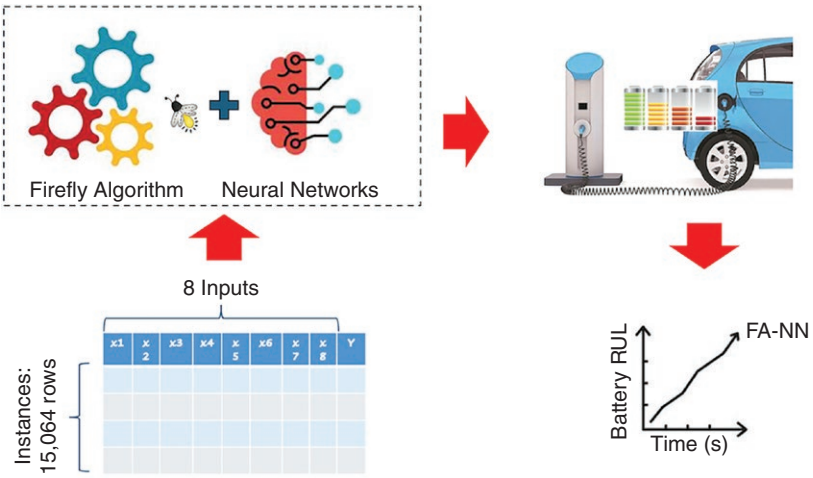

Keywords: battery remaining useful life; firefly algorithm; neural networks; optimization

1. Introduction

The growing popularity of electric vehicle (EV) usage, driven by the increasing focus on sustainable and environmentally friendly transportation solutions, highlights the essential function of energy storage systems, particularly batteries [1–5]. The durability and dependability of batteries play a crucial role in guaranteeing the success and broad acceptance of EVs [6, 7]. Accordingly, precise estimation of the remaining useful life (RUL) of batteries has become a key research focus, enabling proactive maintenance approaches, optimizing battery lifespans, and improving overall system efficiency [8–10]. In addition to estimating the state of charge (SoC), which is important [11], estimating the RUL of batteries is vital due to its direct impact on operational and economic aspects. The unpredictable degradation patterns of batteries

Received: 30 May 2024. **Accepted:** 24 July 2024

require precise forecasting to optimize maintenance schedules and mitigate the risk of unexpected failures. Timely and accurate RUL predictions contribute to enhanced operational planning, reduced downtime, and efficient resource allocation, promoting sustainable practices in the context of EV utilization.

In recent years, the integration of machine-learning techniques such as neural networks (NNs) has significantly advanced and various fields such as finance [12, 13], energy [14–17], cybersecurity [18, 19], manufacturing [20, 21], and healthcare [22–24] as well as automotive [25–27]. Their popularity stems from their capability to learn from data and apply that learning to new scenarios. Consequently, NNs have become a valuable tool for addressing complex problems across different domains, which, in EVs, includes the SoC [28], state of health (SoH) [29], as well RUL [26]. The rapid development in the usage of EVs has opened up numerous research opportunities to support smart cities [30].

In the literature, numerous studies have been presented, addressing the key aspects of battery management systems. Due to the importance of the SoH, the study by Ansari *et al.* [31] demonstrated a hybrid approach that combined jellyfish optimization (JFO) with recurrent neural networks (RNNs). Comparative analysis with other NN models, such as hybrid JFO with other NN models, as well as hybrid particle swarm optimization (PSO) with NN models, indicates the effectiveness of the proposed method for the specific case under consideration. Other investigations on SoH estimation based on RNN can also be found in Hong *et al.* [32] and Chen *et al.* [33].

For the safe handling and effective control of batteries, keeping track of the SoC is crucial. Concerning that matter, a study by Fu *et al.* [34] introduced an improved radial basis function neural network (RBFNN) optimized with the golden section method (GSM) and sparrow search algorithm (SSA). The GSM is employed to determine the ideal number of neurons in the hidden layer, while is utilized to optimize other related parameters of the RBFNN. The effectiveness of the proposed method was proven by its ability to achieve high accuracy. Meanwhile, the use of long short-term memory (LSTM) and a deep-learning neural network (DLNN) for SoC estimation and a random forest for SoH classification was demonstrated by Shibl *et al.* [27]. A similar study that employed a DLNN for SoH, SoC, and RUL estimation were further discussed by Lipu *et al.* [35]. The utilization of LSTM is also evident in work by Zhao *et al.* [36]. In the study, the board learning system algorithm was utilized to replace the input layer of the LSTM NN, aiming to process the collected signals initially. This alteration yields remarkable predictive outcomes.

On the other hand, to achieve an accurate RUL prediction for lithium-ion batteries, a study by Wang *et al.* [37] proposed an adaptive LSTM. The experimental outcomes demonstrate the efficacy and superiority of the proposed prediction approach. Another LSTM-based model for RUL estimation was discussed by Guo *et al.* [38]. The study by Ma *et al.* [39] presented the capability of an improved hybrid PSO–backpropagation neural network (IPSO–BPNN) for the estimation of not only the RUL, but also the SoH. The findings indicate that, in contrast to the standard BPNN approach, the proposed IPSO–BPNN method yields a reduction in both the maximum root mean squared error (RMSE) and the mean absolute error (MAE) for SoC estimation. These outcomes affirm that the IPSO–BPNN method exhibits superior accuracy and validity when compared with the standard BPNN method.

As previously discussed, the integration of optimization algorithms with NNs has demonstrated effectiveness in optimizing the NN hyperparameters. In this study, the application of a hybrid methodology, namely the firefly algorithm–neural network (FA–NN) model, is proposed, to tackle the complexities of RUL prediction. NNs, with their capacity to recognize complex patterns and relationships within data, offer a promising path for tackling the complexities associated with battery behavior and degradation. The FA has been shown to have good convergence properties, often outperforming the genetic algorithm (GA) and PSO in terms of convergence speed and accuracy [40]. Moreover, it has been reported that PSO is prone to getting trapped in local optima in high-dimensional spaces and exhibits a slow convergence rate during the iterative process, while JFO struggles with convergence speed and solution stability [41]. On the other hand, the SSA is documented to easily fall into local optima in the earlier stages and suffers from low accuracy in the later phases [42].

A key advantage of the FA is its adaptive parameter adjustment capability. Unlike many other optimization algorithms, the FA dynamically modifies crucial parameters such as attractiveness and light intensity throughout the optimization process. This inherent adaptability allows the FA to efficiently navigate and respond to changes in the solution space, making it particularly effective for dynamic environments and complex optimization problems. The ability of the algorithm to self-tune these parameters enhances its exploration–exploitation balance, potentially leading to more robust and accurate solutions compared with algorithms with static parameters. In addition, compared with other new optimization algorithms such as JFO, the FA is a more established algorithm with a broader range of applications and studies. By using the capabilities of the FA–NN, this research aims to contribute to the growing body of knowledge surrounding battery health management. The combination of optimization algorithms with NNs is expected to produce more accurate and reliable RUL estimates, promoting a proactive and sustainable approach to battery maintenance in the era of increasing EV adoption. This study not only highlights the importance of RUL estimation, but also emphasizes the crucial role of machine-learning methodologies in influencing the future of battery health management and ensuring the long life and efficiency of energy storage systems in EVs.

The contributions of this paper are outlined as follows:

- Implementing automatic adjustment of NN weights and hidden layer biases using the FA.
- Enhancing the estimation performance of NNs by determining optimal values for the respective hyperparameters.
- Enhancing the accuracy of RUL estimation, specifically targeting a reduction in error rates.

The paper is structured into six main sections to comprehensively address the above objectives. Section 2 provides a background study and reviews existing literature to establish a foundation for the research. Section 3 discusses the estimation process based on NN. In Section 4, the focus is given to the application of the FA in optimization problems. Methodological details are elaborated upon in Section 5. Section 6 presents the results obtained. Finally, in Section 7, the paper concludes by summarizing the findings of the research.

2. Estimation based on NNs

NNs are computational models inspired by the structure and functioning of the human brain, designed to learn and make predictions from data. They consist of layers of interconnected nodes (neurons) and are widely used for various machine-learning tasks, including RUL estimation for batteries [43]. Configuring NNs

involves defining their architecture, which includes specifying the number of layers and the number of neurons in each layer. Common types of layers in NNs include input, hidden, and output layers. The configuration of these layers is crucial and depends on the complexity of the task at hand. More complex tasks might require deeper networks with more hidden layers and neurons.

Optimizing the bias and network weights is a crucial step in training NNs. During the training process, the algorithm adjusts these parameters to minimize the difference between the predicted outputs and the actual values in the training data. The optimization process aims to find the values that result in the most accurate predictions on unseen data. Efficiency in RUL estimation is achieved when the NN is well configured, and the optimization process converges to values that new data generalize well. The network should capture the underlying patterns and relationships in the battery health data, allowing it to make accurate predictions of the RUL. This efficiency is crucial for practical applications, as accurate RUL estimates contribute to effective maintenance planning and resource allocation for battery systems, leading to improved reliability and cost-effectiveness. The use of optimization algorithms such as the FA mentioned earlier (see Section 1) further enhances the efficiency of the NNs in achieving accurate and reliable RUL predictions for batteries.

3. Optimization based on the FA

Introduced by Xin She-Yang [44], the FA was developed based on the flash behavior of fireflies. In nature, bioluminescence plays a crucial role in the courtship rituals of fireflies, serving as the primary means of communication between males and females. The emitted light not only attracts potential mates or prey, but also serves to safeguard their territories, acting as a warning to predators to steer clear of their habitats.

The FA follows the following three principles:

- Fireflies are genderless, and each can be attracted to another firefly without regard to gender.
- The brightness of fireflies is directly proportional to their attractiveness, hence the less-bright firefly tends to move closer to the brighter one in any pair.
- The value of the objective function (fitness value) of the problem being solved is directly linked to the brightness of the firefly.

The brightness I and attractiveness β of the fireflies play a significant role in the FA. When the I is higher, it leads to a better objective function value f. The definition of I is as follows:

$$I = I_0 \times e^{-\gamma \times r_{ij}^2} \tag{1}$$

$$r_{ij} = \|x_i - x_j\| = \sqrt{\sum_{d=1}^{D} (x_{id} - x_{jd})^2} \tag{2}$$

where I_0 represents the brightness of the firefly ($r_{ij} = 0$) and γ is the light absorption coefficient. r_{ij} represents the distance between the fireflies x_i and x_{ij}, which is generally a Euclidean distance. The attractiveness β is defined as follows:

$$\boldsymbol{\beta} = \boldsymbol{\beta}_0 e^{-\gamma r_{ij}^2} \tag{3}$$

where β_0 denotes the attractiveness when $r = 0$. The formula for the movement of a firefly (I) drawn towards another brighter firefly (j) is as follows:

$$x_i^{t+1} = x_i^t + \boldsymbol{\beta}\left(x_j^t - x_i^t\right) + \boldsymbol{\alpha}\,(rand - 0.5) \tag{4}$$

where x_i^t denotes the location of firefly I in the i-th iteration, *rand* is a random number uniformly distributed in [0,1], and a is a constant between 0 and 1.

4. Methodology

This section outlines the implemented methodology, covering diverse elements such as research data and data preparation, data preprocessing, experiment set-up, the proposed FA–NN for the estimation of battery RUL, and examination of the evaluation and benchmark estimation model.

4.1 Research data and data preparation

In this study, a publicly available dataset was utilized, accessible from the Kaggle website [45]. The dataset consists of 15 064 rows, encompassing eight inputs: cycle number (CT), discharge time (s) (DT), decrement from 3.6 to 3.4 V (s) (Dec_3.6-3.4V), maximum voltage during discharge (V) (MVD), minimum voltage during charge (V) (MVC), time at 4.15 V (s) (T_4.15V), time constant current (s) (TCC), and charging time (s) (CT). The sole output variable is the RUL. Table 1 shows a sample of the dataset.

4.2 Data preprocessing

The employed dataset is free from missing values. Before training, linear normalization—specifically min–max normalization—was applied to standardize all input and output values. The primary aim was to prevent larger input values from overshadowing smaller ones, potentially enhancing estimation accuracy. The transformation of all features to a common scale facilitates better convergence and performance of the learning algorithm. The min–max normalization is defined by the following equation:

$$v' = \left(\frac{v - min_a}{max_a - min_a}\right) * (newmax_a - newmin_a) + newmin_a \tag{5}$$

where v' represents the new value for variable v, v is the current value, min_a is the minimum value in the data set, max_a is the maximum value in the dataset, $newmax_a$ is the new maximum value in the dataset, and $newmin_a$ is the new minimum value in the dataset. Min–max normalization transforms a value of v of A into v' within the range [$newmax_a$, $newmin_a$] by solving the above equation. The normalized dataset for the sample in Table 1 is presented in Table 2.

4.3 Training and testing

The dataset is divided into two distinct subsets: a training set, utilized for model fitting, and a testing set, employed for a genuine evaluation of the generalization performance of the model. The split between these subsets follows a proportion of 0.7:0.3. The rationale behind using a 0.7:0.3 split for training and testing data is that this commonly used approach was chosen based on empirical evidence. It often provides a good balance between having enough data for training and sufficient data for testing.

4.4 FA–NN for estimation of battery RUL

Fig. 1 illustrates a hybrid FA–NN model designed for optimizing the weights and biases of a NN in the context of an estimation problem. The NN, featuring eight inputs, one hidden layer, and one output, undergoes a systematic process outlined in the flowchart. This process includes setting the parameters for the NN, loading the normalized dataset of the RUL, defining the training and testing data, and configuring the NN accordingly. Additionally, the FA is employed to optimize the weights and biases of the NN, aiming to minimize the MAE and RMSE between predicted and

Table 1. Sample of dataset.

CI	DT (s)	Dec_3.6-3.4V (s)	MVD (V)	MVC (V)	T_4.15V (s)	TCC (s)	CT (s)	RUL
100	2128.56	768	4.007	3.409	4810.74	5768.34	8901.75	1013
101	2126.97	762	4.006	3.41	4803.51	5768.31	8899.03	1012
102	2125.78	762	4.006	3.411	4796.31	5768.31	8913.22	1011
103	2124.41	764.4	4.006	3.411	4796.38	5768.38	8916.5	1010
104	2122.03	762.4	4.005	3.411	4789.15	5732.34	8875.09	1009
105	2112	759	4.005	3.411	4781.94	5732.34	8892.59	1008
106	2118.81	760.8	4.006	3.413	4774.74	5732.34	8892.44	1007
107	2117.62	756.8	4.006	3.412	4767.51	5732.31	8905.44	1006
108	2115.12	757.2	4.005	3.414	4766.38	5732.38	8854.25	1005
109	2114.31	755.2	4.006	3.414	4760.38	5732.38	8898.38	1004
110	2112.31	753	4.005	3.414	4753.18	5696.38	8870.56	1003
111	2111.19	753	4.005	3.414	4748.38	5696.38	8860.06	1002
112	2100.94	748.8	3.991	3.415	4745.98	6147.88	8766.5	1001
113	2109.81	739.187	4.014	3.674	4690.25	5656	8884.06	1000
115	2124.61	751.2	3.998	3.397	5066.26	6056.26	9425.95	998

*CI, cycle index; DT, discharge time; Dec_3.6-3.4V, decrement 3.6–3.4 V; MVD, maximum voltage discharge; MVC, minimum voltage charge; T_4.15V = time at 4.15 V; TCC, time constant current; CT, charging time; RUL, remaining useful life.

Table 2. Sample of normalized dataset.

CI	DT (s)	Dec_3.6-3.4V (s)	MVD (V)	MVC (V)	T_4.15V (s)	TCC (s)	CT (s)	RUL
0.0874	0.0022	0.4953	0.7303	0.2852	0.0192	0.0065	0.0101	0.8941
0.0883	0.0022	0.4953	0.7295	0.2859	0.0191	0.0065	0.0101	0.8932
0.0891	0.0022	0.4953	0.7295	0.2867	0.0191	0.0065	0.0101	0.8923
0.0900	0.0022	0.4953	0.7295	0.2867	0.0191	0.0065	0.0101	0.8914
0.0909	0.0022	0.4953	0.7288	0.2867	0.0191	0.0065	0.0101	0.8906
0.0918	0.0022	0.4953	0.7288	0.2867	0.0190	0.0065	0.0101	0.8897
0.0927	0.0022	0.4953	0.7295	0.2881	0.0190	0.0065	0.0101	0.8888
0.0936	0.0022	0.4953	0.7295	0.2874	0.0190	0.0065	0.0101	0.8879
0.0944	0.0022	0.4953	0.7288	0.2889	0.0190	0.0065	0.0100	0.8870
0.0953	0.0022	0.4953	0.7295	0.2889	0.0189	0.0065	0.0101	0.8861
0.0962	0.0022	0.4953	0.7288	0.2889	0.0189	0.0065	0.0101	0.8853
0.0971	0.0022	0.4953	0.7288	0.2889	0.0189	0.0065	0.0101	0.8844
0.0980	0.0022	0.4953	0.7182	0.2896	0.0189	0.0070	0.0099	0.8835
0.0989	0.0022	0.4953	0.7356	0.4805	0.0187	0.0064	0.0101	0.8826
0.1006	0.0022	0.4953	0.7235	0.2763	0.0202	0.0069	0.0107	0.8808

actual RUL values. The optimization involves setting FA parameters, specifying the number of iterations and population size, and iterating until a termination criterion is met or the maximum number of iterations is reached. The final step involves testing the trained NN on unseen data, calculating the MAE and RMSE, recording the best result, and concluding the process by reporting the overall performance of the FA–NN model.

4.5 Properties setting

Prior to experimental processes, the properties of the proposed technique and the identified techniques are set, which is tabulated in Table 3. For the autoregressive integrated moving average (ARIMA), the values of p [the order of the autoregressive (AR) term], d (the degree of differencing), and q [the order of the moving average (MA) term] are set based on experimental data, within the ranges of 0–5, 0–1, and 0–5, respectively.

4.6 Evaluation

The selection of a suitable performance evaluation metric is essential for validating the results obtained in the experiment. In this study, two quantitative evaluation metrics are employed: the MAE and the RMSE. The formulas for the MAE and RMSE are illustrated in the following equations:

$$MAE = \frac{1}{N}\sqrt{\sum_{i=1}^{N} |y(i) - \hat{y}(i)|} \tag{6}$$

$$RMSE = \sqrt{\frac{\sum_{i=1}^{N} \|y(i) - \hat{y}(i)\|^2}{N}} \tag{7}$$

where N represents the data length of the battery RUL under evaluation, with $y(i)$ and $\hat{y}(i)$ denoting the target and estimated battery RUL, respectively. These metrics measure how close the

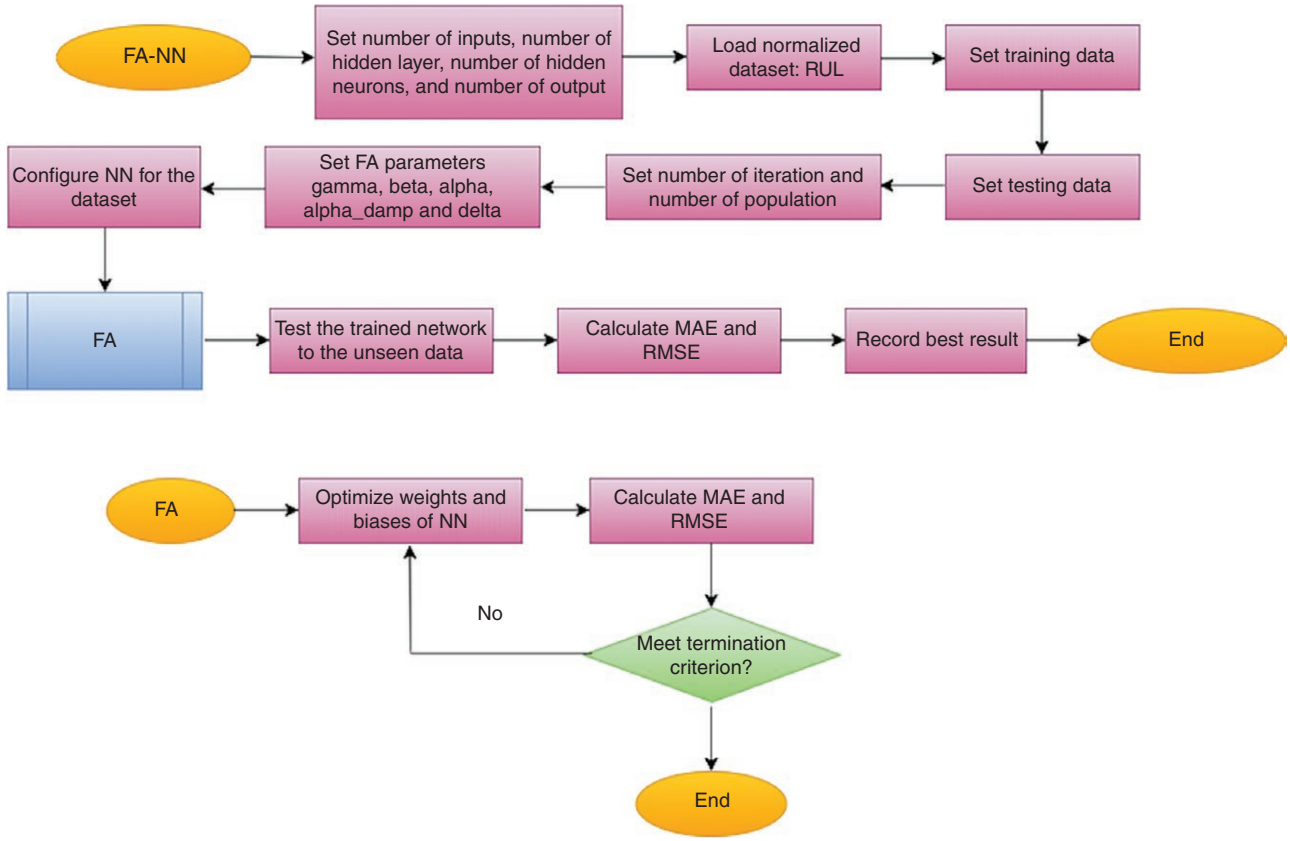

Figure 1. FA–NN for battery RUL estimation.

Table 3. Properties of prediction techniques utilized.

Properties	FA	HSA	CA	NN
Population size	30	30	30	–
Maximum iteration	1000	1000	1000	–
Light absorption coefficient, γ	1	–	–	–
Attraction coefficient base value, *β*	2	–	–	–
Mutation coefficient, α	0.2	–	–	–
Harmony memory consideration rate	–	0.9	–	–
Pitch adjustment rate	–	0.1	–	–
Acceptance rate	–	–	0.3	–
Number of hidden layers	–	–	–	1
Number of neurons	–	–	–	9

predictions of the model are to the actual values. Lower values indicate better performance.

4.6 Benchmark estimation models

To facilitate comparison, the FA–NN is assessed alongside other models, including the NN hybridized with the harmony search algorithm (HSA) [46], cultural algorithm (CA) [47], and ARIMA.

4.6.1 *HSA*

The HSA is a heuristic optimization algorithm inspired by the improvisation process of musicians in a jazz ensemble [46]. The algorithm mimics the process by which musicians harmonize their notes to find an optimal solution to a problem. The algorithm begins with the initialization phase, in which the original population of potential solutions, called "harmonies," is initialized. Harmonies are selected from the population based on their fitness values such that the better-performing solutions are more likely to be included in the harmony memory.

New harmonies are generated by adjusting the pitches (values) of existing harmonies. This process embodies the balance between exploration and exploitation in the search for improved solutions.

4.6.2 *CA*

The CA [47] belongs to the category of evolutionary computation, encompassing a knowledge component called the belief space alongside the population component. In this context, the CA can be seen as an expansion of the conventional GA. Similarly to many other metaheuristic algorithms, the CA initiates with an initialization phase, involving the set-up of candidate solutions

and the belief space representing cultural knowledge. During the evaluation phase, the fitness or objective function of individuals in the population is assessed, and the belief space is updated based on their performance and experiences. Like the GA [48], the CA includes crossover and mutation operators to generate new candidate solutions. In the selection phase, individuals are chosen based on their fitness values or a combination of fitness and cultural knowledge.

4.6.3 *ARIMA*

The ARIMA is a widely used time series forecasting model. It combines autoregression (AR), differencing (I), and MA to capture temporal dependencies and patterns in sequential data, making it effective for predicting future values based on historical observations.

5. Results and discussion

To evaluate the feasibility and robustness of the proposed method for battery RUL estimation, the FA–NN was initially tested with various values for the number of hidden neurons. The number of hidden neurons is a hyperparameter that controls the complexity of the NN. It affects the ability of the model to learn from the data and generalize to new data. This was conducted to ensure that the estimation model avoids encountering underfitting or overfitting issues. Subsequently, the best results obtained were compared with those from an identified benchmark estimation model.

5.1 Assessing NN configurations for battery RUL estimation using the FA–NN

Table 4 presents the outcomes of the FA–NN estimation model under different configurations of hidden neurons (7, 9, and 11). The configuration utilizing nine hidden neurons excels in all metrics, suggesting an optimal balance between bias and variance. This configuration strikes a harmonious middle ground, steering clear of both overfitting and underfitting by being neither excessively complex nor overly simplistic. Overfitting occurs when the model is overly complex, fitting noise in the training data and resulting in poor generalization and high variance. Conversely, underfitting happens when the model is too simple, failing to capture underlying patterns in the data, leading to mediocre performance and high bias.

The configuration with seven hidden neurons may indicate underfitting, as evidenced by its highest MAE and RMSE values. Conversely, the configuration with 11 hidden neurons might suggest overfitting, as indicated by increased error metrics compared with 9 neurons, especially a significantly higher maximum error. The maximum error represents the largest difference between the prediction of the model and the actual value for any data point, illustrating the potential unreliability of the model and the likelihood of producing highly inaccurate results for certain inputs.

5.2 Comparison of the FA–NN with benchmarking hybrid estimation algorithms

Table 5 provides a comparison of four identified estimation models employed for estimating battery RUL: FA–NN, CA–NN, ARIMA, and HSA–NN. The FA–NN emerges as the most accurate model for estimating battery RUL, displaying the lowest values for MAE, RMSE, and maximum error among all models. The ARIMA exhibits significantly higher errors in all three metrics compared with the FA–NN, HSA–NN, and CA–NN. Being a statistical model that captures temporal dependencies, the ARIMA is inherently limited in its ability to model non-linear relationships or handle data with complex non-linear structures. The CA–NN demonstrates a significantly lower MAE and RMSE than the HSA–NN but a considerably higher maximum error, suggesting potential sensitivity to outliers or noise in the data, leading to larger errors for certain inputs.

Fig. 2 visualizes a comparative analysis of battery RUL estimation produced by the FA–NN and identified algorithms, namely the HSA–NN, CA–NN, and ARIMA. Each subplot corresponds to one model while the close-up figure is illustrated in Fig. 3. On the top-left (actual vs. FA–NN), the dashed line represents the actual RUL, while the solid line represents the RUL predicted by the FA–NN model. The predictions of the FA–NN model closely follow the actual RUL, with minimal deviation. On the top-right (actual vs. HSA–NN), the dashed line represents the actual RUL and the other solid line represents the RUL predicted by the HSA–NN model. While the predictions of the HSA–NN model generally align with the actual RUL, closer inspection reveals some fluctuations (see Fig. 3). In the bottom-left (actual vs. CA–NN), the dashed line represents the actual RUL and another solid line represents the RUL predicted by the CA–NN model. The CA–NN model shows a good fit overall but with more noticeable fluctuations compared with the FA–NN model. Finally, in the bottom-right (actual vs. ARIMA), the dashed line represents the actual RUL and a different solid line represents the RUL predicted by the ARIMA model. The predictions of the ARIMA model significantly deviate from the actual RUL, especially towards the end of the timeline, indicating lower accuracy compared with the NN-based models. Overall, the FA–

Table 4. FA–NN with 7, 9, and 11 hidden neurons.

Number of hidden neurons	7	9	11
MAE	2.9707	**2.5371**	2.7645
RMSE	3.6968	**2.9488**	3.1852
Maximum error	35.4748	**34.3737**	68.2774

Table 5. Estimation of battery RUL: FA–NN vs. HAS–NN vs. CA–NN vs. ARIMA.

	FA–NN	HSA–NN	CA–NN	ARIMA
MAE	**2.5371**	22.0583	9.1189	494.6275
RMSE	**2.9488**	34.5154	22.4646	584.3098
Maximum error	**34.3737**	490.3125	827.0163	1.16e + 03

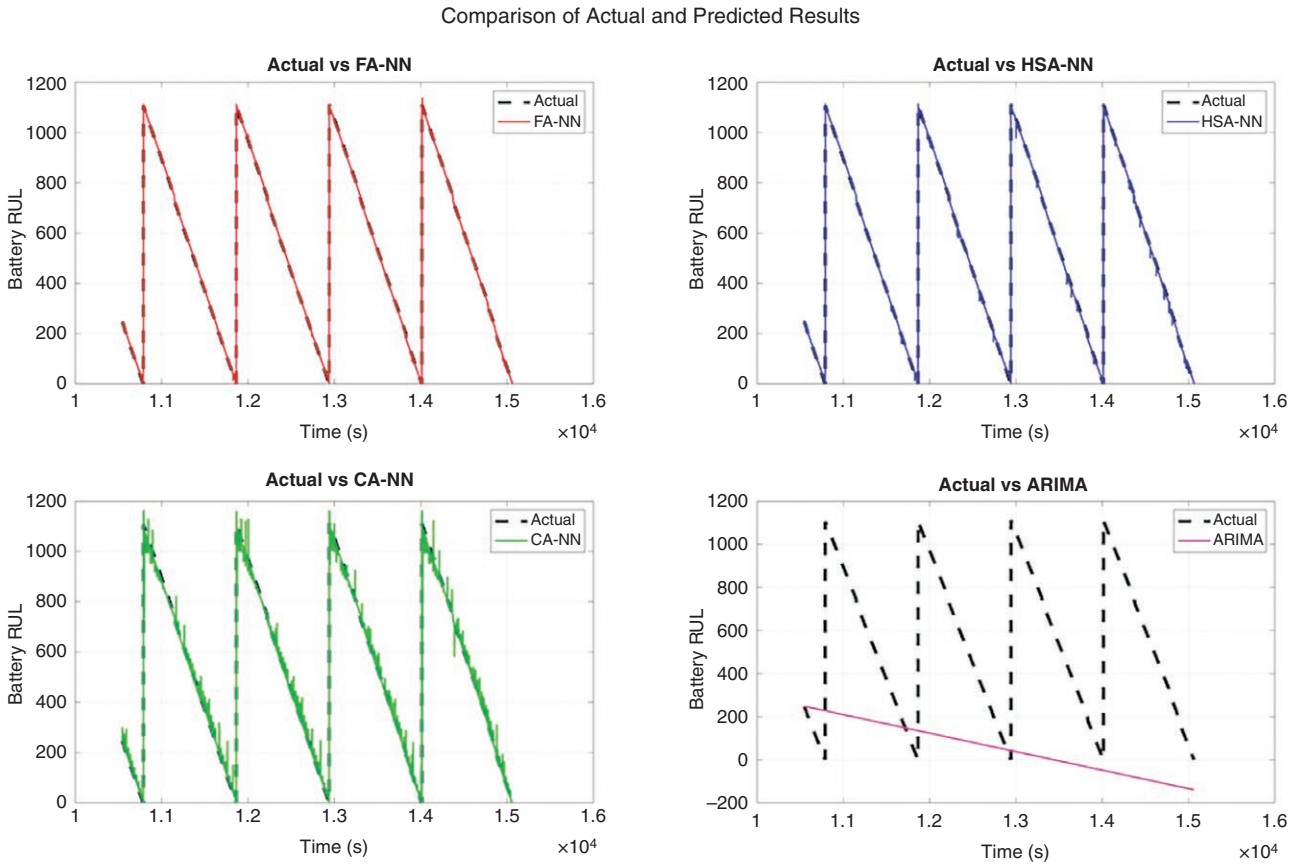

Figure 2. Comparative analysis of battery RUL estimation: FA–NN, HSA–NN, CA–NN, and ARIMA models.

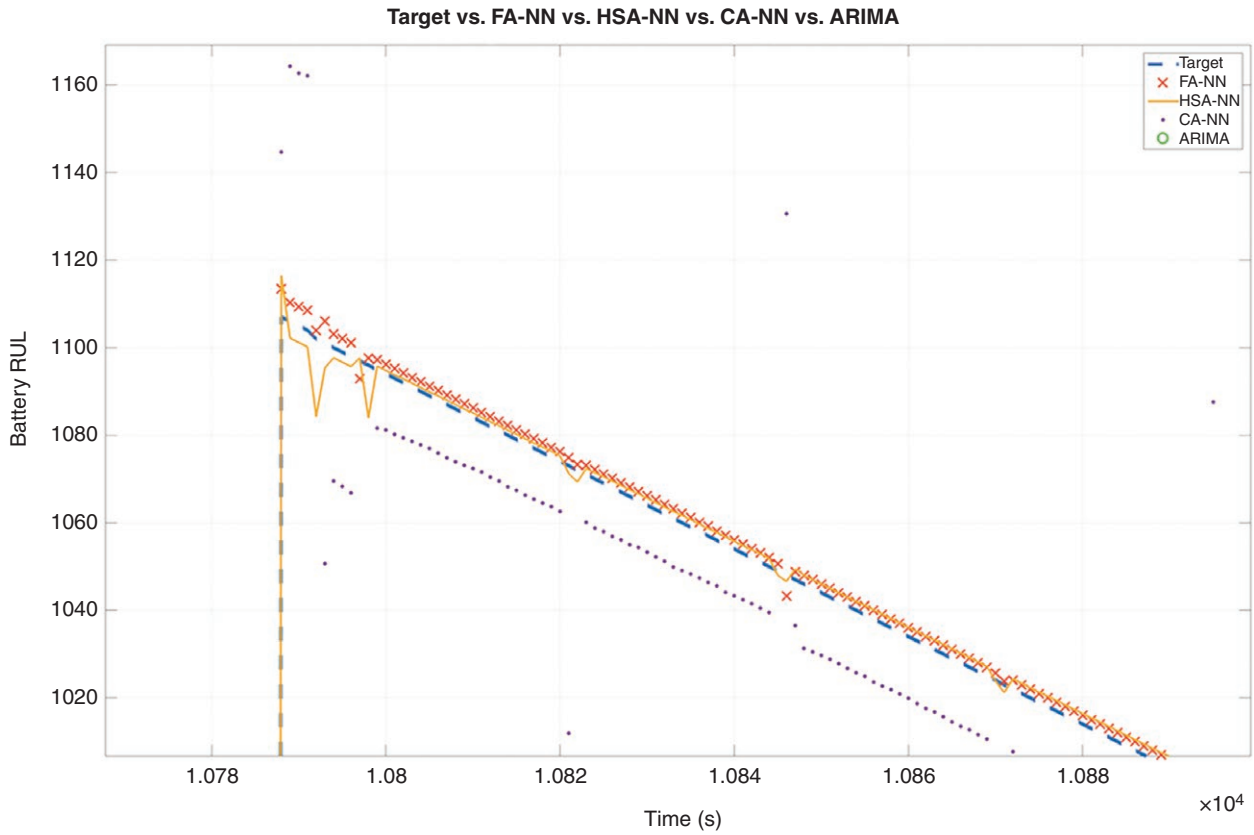

Figure 3. Zoomed-in comparison of battery RUL estimation: FA–NN, HSA–NN, CA–NN, and ARIMA models.

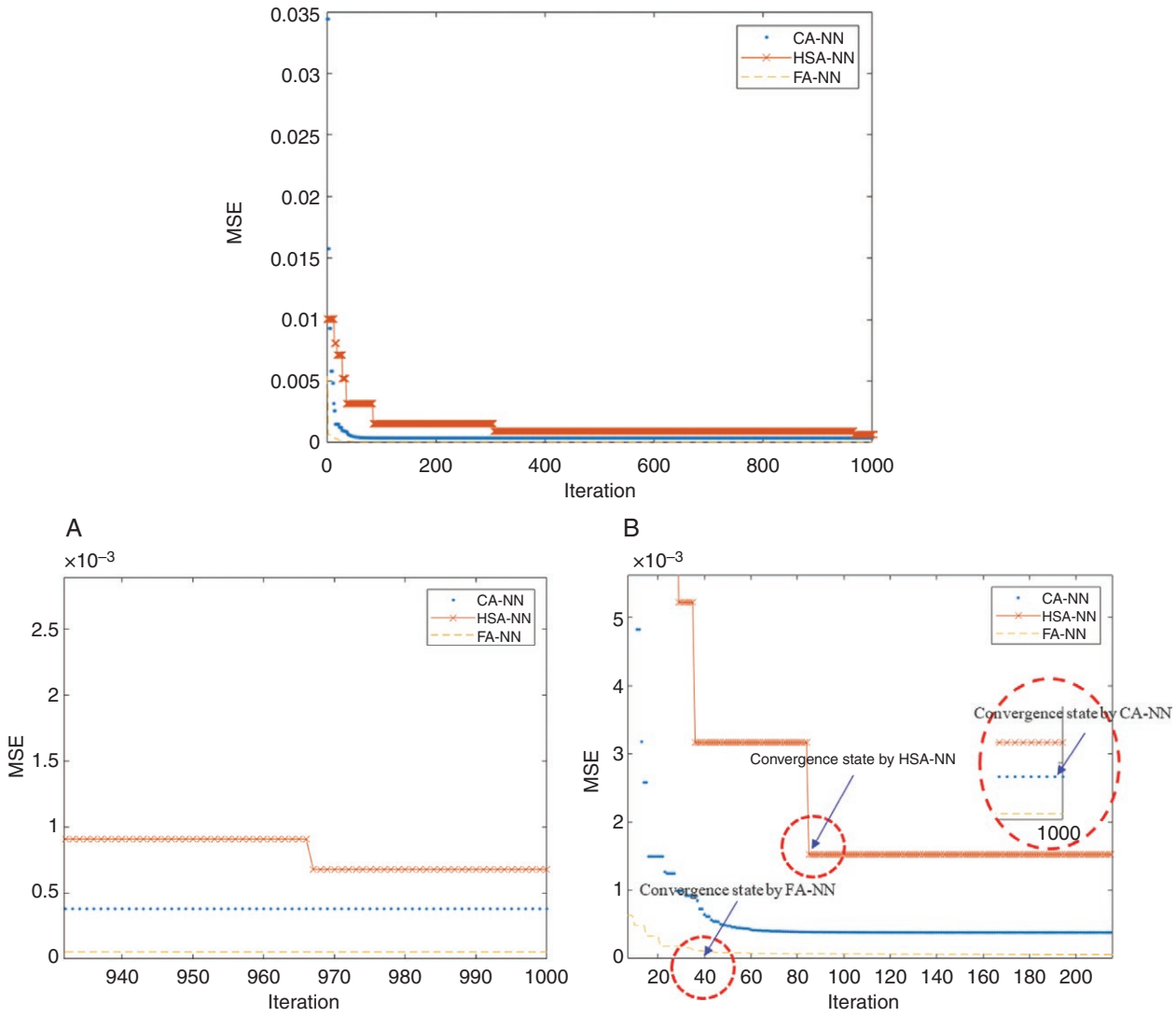

Figure 4. Comparison of convergence rates for battery RUL. (a) Zoomed-in comparison of convergence rates for battery RUL. (b) Zoomed-in comparison of convergence rates for battery RUL.

Table 6. Statistical comparison of the FA–NN method against HSA–NN, CA–NN, and ARIMA methods using paired sample tests.

Methods	P-value
FA–NN vs. HSA–NN	**0.0000**
FA–NN vs. CA–NN	**0.0000**
FA–NN vs. ARIMA	**0.0000**

NN model provides the most accurate RUL predictions, showing the closest alignment with the actual RUL data.

Fig. 3 shows the zoom-in of the produced estimation values by the FA–NN, HSA–NN, and CA–NN. From the figure, it is evident that the FA–NN exhibits the most accurate predictions among the three models, as it closely aligns with the target RUL values. In contrast, the HSA–NN demonstrates significant deviation from the target RUL values, displaying higher errors as tabulated in Table 4. Meanwhile, the CA–NN also diverges from the target RUL but outperforms the HSA–NN in terms of MAE and RMSE. The effectiveness of the FA–NN is attributed to the optimization capabilities of the FA, while poor performance by the HSA–NN may be due to suboptimal parameter tuning or convergence issues. Moderate performance by the CA–NN suggests that there is room for improvement. The ARIMA model is not shown in this zoomed-in figure due to its large deviations from the target RUL values, highlighting its lower accuracy compared with the NN-based models.

Fig. 4 illustrates the convergence rates of three algorithms: FA–NN, CA–NN, and HSA–NN; Fig. 4a and b visualizes a close-up of Fig. 4. The assessment of the performance of each algorithm is based on the mean squared error (MSE) metric. The *x*-axis denotes iterations, spanning from 1 to 1000, while the *y*-axis represents the MSE. The FA–NN (depicted by the dashed line) exhibits rapid convergence to an MSE of 0 around the fortieth iteration, maintaining stability thereafter. In terms of algorithm performance, the FA–NN achieves the lowest MSE (0.0000) and converges early, by approximately the fortieth iteration. Meanwhile, the HSA–NN was able to converge at approximately the eighty-fifth iteration. Unfortunately, the performance of the CA–NN did not significantly improve or it converged to a lower error during these iterations.

The FA–NN effectively optimizes NN weights and biases, promoting quick learning and convergence. The thorough exploration of the solution space by the algorithm allows the speedy

identification of optimal weights. The early convergence observed can be credited to the adaptive search behavior inherent in the FA.

Table 6 presents a statistical comparison of the FA–NN method against three other methods: HSA–NN, CA–NN, and ARIMA. The comparison is based on *P*-values derived from paired sample tests. Notably, all *P*-values are reported as 0.0000, indicating statistically significant differences between the FA–NN and each of the other methods across all comparisons. This consistency suggests that the FA–NN performs distinctly from the other approaches.

6. Conclusion

In conclusion, this study introduces and assesses the efficacy of a hybrid approach, FA–NN, for estimating the RUL of batteries. By leveraging the FA as an optimizer to fine-tune NN parameters, the proposed FA–NN model demonstrates enhanced accuracy in battery RUL predictions. Through a comprehensive comparative analysis against the HSA–NN, CA–NN, and ARIMA, it becomes evident that the FA–NN outperforms these models in terms of both MAE and RMSE. The FA–NN achieved the lowest MAE of 2.5371 and RMSE of 2.9488. In comparison, the HSA–NN had an MAE of 22.0583 and RMSE of 34.5154, while the CA–NN showed an MAE of 9.1189 and RMSE of 22.4646. The ARIMA model performed the least favorably with an MAE of 494.6275 and RMSE of 584.3098. The superior predictive capabilities of the FA–NN are further emphasized by its significantly smaller maximum errors compared with those of the other identified algorithms, as its maximum error was 34.3737, which was substantially lower than those of the HSA–NN (490.3125), CA–NN (827.0163), and ARIMA (1160.0000). This research contributes valuable insights into the field of battery health management, affirming the effectiveness of the FA–NN methodology as a promising and reliable solution for accurate RUL predictions.

Looking ahead, future work will concentrate on refining and optimizing the FA–NN methodology. Exploring the incorporation of additional data sources or advanced NN architectures could enhance the predictive capabilities of the model. Moreover, conducting real-world experiments and validations with diverse battery types and operational conditions would strengthen the generalizability of the proposed approach. This research lays the foundation for ongoing advancements in battery prognostics and provides a pathway for the continued evolution of RUL estimation methodologies.

Author contributions

Zuriani Mustaffa (Conceptualization [Equal], Data curation [Equal], Methodology [Equal], Writing—original draft [Equal]), and Mohd Herwan Sulaiman (Formal analysis [Equal], Validation [Equal], Writing—review & editing [Equal])

Conflict of interest statement

The authors declare no competing interests.

Funding

This research is supported by Universiti Malaysia Pahang Al-Sultan Abdullah, grant number: RDU220379.

Data availability

The datasets are available at https://www.kaggle.com/code/ahmedhatem404/rul-analysis-machine-learning/notebook.

References

[1] Miranda MHR, Silva FL, Lourenço MAM *et al*. Particle swarm optimization of Elman neural network applied to battery state of charge and state of health estimation. *Energy* 2023;**285**:129503. https://doi.org/10.1016/j.energy.2023.129503

[2] Liu L. Data-driven prognosis of multiscale and multiphysics complex system anomalies: its application to lithium-ion batteries failure detection. *J Electrochem Soc* 2023;**170**:050525. https://doi.org/10.1149/1945-7111/acd300

[3] Kouhestani HS, Liu L, Wang R *et al*. Data-driven prognosis of failure detection and prediction of lithium-ion batteries. *J Storage Mater* 2023;**70**:108045. https://doi.org/10.1016/j.est.2023.108045

[4] Liu L. (Digital Presentation) Data-driven prognosis of lithium-ion batteries thermal runaway early warning and detection. In: *ECS Meeting Abstracts 2023*; MA2023-01: 2779. Boston, MA, USA. https://doi.org/10.1149/MA2023-0172779mtgabs

[5] Kouhestani HS, Yi X, Qi G *et al*. Prognosis and health management (PHM) of solid-state batteries: perspectives, challenges, and opportunities. *Energies* 2022;**15**:6599. https://doi.org/10.3390/en15186599

[6] Nyamathulla S, Dhanamjayulu C. A review of battery energy storage systems and advanced battery management system for different applications: challenges and recommendations. *J Storage Mater* 2024;**86**:111179. https://doi.org/10.1016/j.est.2024.111179

[7] Singh A, Pal K, Vishwakarma CB. State of charge estimation techniques of Li-ion battery of electric vehicles. *e-Prime—Adv Electr Eng* 2023;**6**:100328. https://doi.org/10.1016/j.prime.2023.100328

[8] Duan W, Song S, Xiao F *et al*. Battery SoH estimation and RUL prediction framework based on variable forgetting factor online sequential extreme learning machine and particle filter. *J Storage Mater* 2023;**65**:107322. https://doi.org/10.1016/j.est.2023.107322

[9] Xu Z, Xie N, Li K. Remaining useful life prediction for lithium-ion batteries with an improved grey particle filter model. *J Storage Mater* 2024;**78**:110081. https://doi.org/10.1016/j.est.2023.110081

[10] Wang Z, Liu Y, Wang F *et al*. Capacity and remaining useful life prediction for lithium-ion batteries based on sequence decomposition and a deep-learning network. *J Storage Mater* 2023;**72**:108085. https://doi.org/10.1016/j.est.2023.108085

[11] Liu X, Gao Y, Marma K *et al*. Advances in the study of techniques to determine the lithium-ion battery's state of charge. *Energies* 2024;**17**:1643. https://doi.org/10.3390/en17071643

[12] Lei YT, Ma CQ, Ren YS *et al*. A distributed deep neural network model for credit card fraud detection. *Fin Res Lett* 2023;**58**:104547. https://doi.org/10.1016/j.frl.2023.104547

[13] Karthikeyan T, Govindarajan M, Vijayakumar V. An effective fraud detection using competitive swarm optimization based deep neural network. *Meas: Sens* 2023;**27**:100793. https://doi.org/10.1016/j.measen.2023.100793

[14] Almarzooqi AM, Maalouf M, El-Fouly THM *et al*. A hybrid machine-learning model for solar irradiance forecasting. *Clean Energy* 2024;**8**:100–10. https://doi.org/10.1093/ce/zkad075

[15] Demir H. Simulation and forecasting of power by energy harvesting method in photovoltaic panels using artificial neural network. *Renew Energy* 2024;**222**:120017. https://doi.org/10.1016/j.renene.2024.120017

[16] Wazirali R, Yaghoubi E, Abujazar MSS *et al*. State-of-the-art review on energy and load forecasting in microgrids using artificial neural networks, machine learning, and deep learning techniques. *Electr Power Syst Res* 2023;**225**:109792. https://doi.org/10.1016/j.epsr.2023.109792

[17] Wang X, Razmjooy S. Improved Giza pyramids construction algorithm for modify the deep neural network-based method for energy demand forecasting. *Heliyon* 2023;**9**:e20527. https://doi.org/10.1016/j.heliyon.2023.e20527

[18] Zhang Y, Feng F, Liao Z *et al*. Universal backdoor attack on deep neural networks for malware detection. *Appl Soft Comput* 2023;**143**:110389. https://doi.org/10.1016/j.asoc.2023.110389

[19] Fiza TVGS, Kumar ATAK, Devi VS *et al*. Improved chimp optimization algorithm (ICOA) feature selection and deep neural network framework for Internet of Things (IOT) based android malware detection. *Meas: Sens* 2023;**28**:100785. https://doi.org/10.1016/j.measen.2023.100785

[20] Gao P, Wang J, Zhong R *et al*. Neuron Synergy based explainable neural network for manufacturing cycle time forecasting. *J Manuf Syst* 2023;**71**:695–706. https://doi.org/10.1016/j.jmsy.2023.10.011

[21] Rumbe G, Hamasha M, Al-Mashaqbeh S. A comparison of holts-winter and artificial neural network approach in forecasting: a case study for tent manufacturing industry. *Results Eng* 2024;**21**:101899. https://doi.org/10.1016/j.rineng.2024.101899

[22] Ayadi MG, Mezni H, Alnashwan R *et al*. Effective healthcare service recommendation with network representation learning: a recursive neural network approach. *Data Knowl Eng* 2023;**148**:102233. https://doi.org/10.1016/j.datak.2023.102233

[23] Patel SK. Improving intrusion detection in cloud-based healthcare using neural network. *Biomed Signal Proc Control* 2023;**83**:104680. https://doi.org/10.1016/j.bspc.2023.104680

[24] Chen TCT, Wu HC, Chiu MC. A deep neural network with modified random forest incremental interpretation approach for diagnosing diabetes in smart healthcare. *Appl Soft Comput* 2024;**152**:111183. https://doi.org/10.1016/j.asoc.2023.111183

[25] Korkmaz M. SoC estimation of lithium-ion batteries based on machine learning techniques: a filtered approach. *J Storage Mater* 2023;**72**:108268. https://doi.org/10.1016/j.est.2023.108268

[26] Olabi AG, Abdelghafar AA, Soudan B *et al*. Artificial neural network driven prognosis and estimation of lithium-ion battery states: current insights and future perspectives. *Ain Shams Eng J* 2024;**15**:102429. https://doi.org/10.1016/j.asej.2023.102429

[27] Shibl MM, Ismail LS, Massoud AM. A machine learning-based battery management system for state-of-charge prediction and state-of-health estimation for unmanned aerial vehicles. *J Storage Mater* 2023;**66**:107380. https://doi.org/10.1016/j.est.2023.107380

[28] Mehta C, Sant AV, Sharma P. Optimized ANN for LiFePO4 battery charge estimation using principal components based feature generation. *Green Energy Intell Transp* 2024;**3**:100175. https://doi.org/10.1016/j.geits.2024.100175

[29] Das K, Kumar R. Electric vehicle battery capacity degradation and health estimation using machine-learning techniques: a review. *Clean Energy* 2023;**7**:1268–81. https://doi.org/10.1093/ce/zkad054

[30] Ragab A, Osama A, Ramzy A. Simulation of the environmental impact of industries in smart cities. *Ain Shams Eng J* 2023;**14**:102103. https://doi.org/10.1016/j.asej.2022.102103

[31] Ansari S, Ayob A, Lipu MSH *et al*. Jellyfish optimized recurrent neural network for state of health estimation of lithium-ion batteries. *Expert Syst Appl* 2024;**238**:121904. https://doi.org/10.1016/j.eswa.2023.121904

[32] Hong J, Chen Y, Chai Q *et al*. State-of-health estimation of lithium-ion batteries using a novel dual-stage attention mechanism based recurrent neural network. *J Storage Mater* 2023;**72**:109297. https://doi.org/10.1016/j.est.2023.109297

[33] Chen Z, Zhao H, Zhang Y *et al*. State of health estimation for lithium-ion batteries based on temperature prediction and gated recurrent unit neural network. *J Power Sources* 2022;**521**:230892. https://doi.org/10.1016/j.jpowsour.2021.230892

[34] Fu B, Wang W, Li Y *et al*. An improved neural network model for battery smarter state-of-charge estimation of energy-transportation system. *Green Energy Intell Transp* 2023;**2**:100067. https://doi.org/10.1016/j.geits.2023.100067

[35] Lipu MSH, Ansari A, Miah MS *et al*. Deep learning enabled state of charge, state of health and remaining useful life estimation for smart battery management system: methods, implementations, issues and prospects. *J Storage Mater* 2022;**55**:105752. https://doi.org/10.1016/j.est.2022.105752

[36] Zhao S, Zhang C, Wang Y. Lithium-ion battery capacity and remaining useful life prediction using board learning system and long short-term memory neural network. *J Storage Mater* 2022;**52**:104901. https://doi.org/10.1016/j.est.2022.104901

[37] Wang Z, Liu N, Chen C *et al*. Adaptive self-attention LSTM for RUL prediction of lithium-ion batteries. *Inf Sci* 2023;**635**:398–413. https://doi.org/10.1016/j.ins.2023.01.100

[38] Guo X, Wang K, Yao S *et al*. RUL prediction of lithium-ion battery based on CEEMDAN-CNN BiLSTM model. *Energy Rep* 2023;**9**:1299–306. https://doi.org/10.1016/j.egyr.2023.05.121

[39] Ma Y, Yao M, Liu H *et al*. State of health estimation and remaining useful life prediction for lithium-ion batteries by improved particle swarm optimization-back propagation neural network. *J Storage Mater* 2022;**52**:104750. https://doi.org/10.1016/j.est.2022.104750

[40] Li J, Wei X, Li B *et al*. A survey on firefly algorithms. *Neurocomputing* 2022;**500**:662–78. https://doi.org/10.1016/j.neucom.2022.05.100

[41] Abdelqawee IM, Emam AW, ElBages MS *et al*. An improved energy management strategy for fuel cell/battery/supercapacitor system using a novel hybrid jellyfish/particle swarm/BAT optimizers. *J Energy Storage* 2023;**57**:106276. https://doi.org/10.1016/j.est.2022.106276

[42] Zhou X, Hu W, Zhang Z *et al*. Adaptive mutation sparrow search algorithm-Elman-AdaBoost model for predicting the deformation of subway tunnels. *Underground Space* 2024;**17**:320–60. https://doi.org/10.1016/j.undsp.2023.09.014

[43] Kurucan M, Özbaltan M, Yetgin Z *et al*. Applications of artificial neural network based battery management systems: a literature review. *Renew Sustain Energy Rev* 2024;**192**:114262. https://doi.org/10.1016/j.rser.2023.114262

[44] Yang XS. *Nature-Inspired Metaheuristic Algorithms*. 2nd revised edn. Bristol, UK: Luniver Press, 2010.

[45] Aboelkhair AH, Hamed NA, Reda O *et al*. *RUL Analysis & Machine Learning*. https://www.kaggle.com/code/ahmedhatem404/rul-analysis-machine-learning/notebook (22 January 2024, date last accessed).

[46] Geem ZW, Kim JH, Loganathan GV. A new heuristic optimization algorithm: harmony search. *Simulation* 2001;**76**:60–8. https://doi.org/10.1177/003754970107600201

[47] Reynolds RG. *An introduction to cultural algorithm. In: Proceedings of the 3rd Annual Conference on Evolutionary Programming*. San Diego, California, USA: World Scientific, 1994.

[48] Haupt RL, Haupt SE. *Practical Genetic Algorithms*. 2nd edn. Hoboken, NJ, USA: John Wiley & Sons, Inc., 2004.